Measuring Metabolic Function with PET: Technical Considerations

Terry F. Brown, Nicholas J. Yasillo, Jason Chou, John T. Metz, Chin-Tu Chen and Malcolm D. Cooper

Franklin McLean Memorial Research Institute, Department of Radiology, The University of Chicago, Chicago, Illinois

Objective: The purpose of this study was to determine the magnitude of methodologic errors when PET is used for the quantitative measurement of regional cerebral glucose metabolism ($rCMR_{glu}$).

Methods: Performance of the analytic tests, which are the variables in the quantitative measurement of $rCMR_{glu}$ with PET, was evaluated.

Results: For the scanner we evaluated, failure to perform daily calibration factor calculations was the single largest source of error. In addition, any variation in the accuracy or precision of patient plasma sample pipetting or plasma glucose level determinations, will result in corresponding changes in $rCMR_{glu}$.

Conclusions: Quantitative measurement of $rCMR_{glu}$ with PET requires close attention to laboratory skills, especially proper operation and maintenance of pipettes.

Key Words: positron emission tomography; quality control; fluorine-18-FDG

J Nucl Med Technol 1995; 23:176–180

PET has been used to identify characteristic abnormalities of cerebral glucose metabolism in patients with partial epilepsy (*1*), dementia (*2*) and movement disorders (*3*), even when the x-ray computed tomography (CT) and magnetic resonance imaging (MRI) studies of these patients are normal. While some of these abnormalities can be detected by qualitative analysis, most require a quantitative analysis of the PET image data utilizing a compartmental model which describes the process of cerebral glucose metabolism (Fig. 1).

At the University of Chicago, we use the method of Hutchins et al. (*4*) to calculate the rate of regional cerebral glucose metabolism ($rCMR_{glu}$). This method utilizes the standard nuclear medicine technique for the measurement of substrate accumulation to quantitate a metabolic process. A trace amount of ^{18}F-2-fluoro-2-deoxyglucose ([^{18}F]-FDG) is added to the plasma pool via intravenous injection. The amount administered being small enough to avoid altering the steady state of glucose transport and metabolism. We then carefully measure the clearance from the plasma pool and image the plasma and metabolized pools in the brain. However, because measurements of radioactivity concentrations cannot differentiate between [^{18}F]-FDG and [^{18}F]-FDG-6-phosphate in tissue, an equation is required to separate the two:

$$rCMR_{glu} = \frac{C_g}{LC} \times \frac{k_1 \times k_3}{k_2 + k_3} \times \left[\frac{C_i(T)}{C'_E(T) + C'_M(T)}\right]. \quad \text{Eq. 1}$$

In this equation, C_g is the plasma glucose concentration; LC is the lumped constant which corrects for slight differences between glucose and deoxyglucose metabolism; k_1, k_2 and k_3 are the metabolic rate constants defined by Sokoloff (*5*); $C_i(T)$ is the total ^{18}F concentration in the tissue measured with the PET scanner at time T; and $C'_E(T)$ and $C'_M(T)$ represent the concentrations of ^{18}F-FDG free in the tissue and ^{18}F-FDG-6-phosphate in the tissue, respectively, at time T. $C'_E(T)$ and $C'_M(T)$ are calculated by convolving (*6*) the plasma activity time curve (C_p) with complex exponential expressions containing the rate constants k_1–k_4. $C_i(T)$ is measured with the PET scanner in units of cps/pixel. This value is converted to cps/ml utilizing a calibration factor obtained from a phantom study:

$$C_i(T) = \frac{\text{subject cps/pixel in PET image}}{\left(\frac{\text{phantom cps/pixel in PET image}}{\text{aliquot from phantom cps/ml in well counter}}\right)}. \quad \text{Eq. 2}$$

Using the lumped constant of 0.418 ± 0.058 and the mean phosphorylation rate of 0.0243 ± 0.0039 min^{-1} reported by Huang et al. (*7*), Equation 1 becomes:

$$rCMR_{glu} = \frac{C_g}{0.05813} \times \left[\frac{C_i(T)}{C'_E(T) + C'_M(T)}\right]. \quad \text{Eq. 3}$$

We are then able to obtain a metabolic rate by measuring only: C_g, C_p, and $C_i(T)$. Table 1 summarizes the possible sources of error associated with the measurement of each of these variables. A limitation of this type of quantitative analysis is the reproducibility with which each of these variables can be measured. In other words, are differences in measured metabolic rates due to changes in the subject, or

For correspondence or reprints contact: Terry F. Brown, BS, CNMT, The University of Chicago, Franklin McLean Memorial Research Institute, MC 1037, 5841 S. Maryland Ave., Chicago, IL 60637.

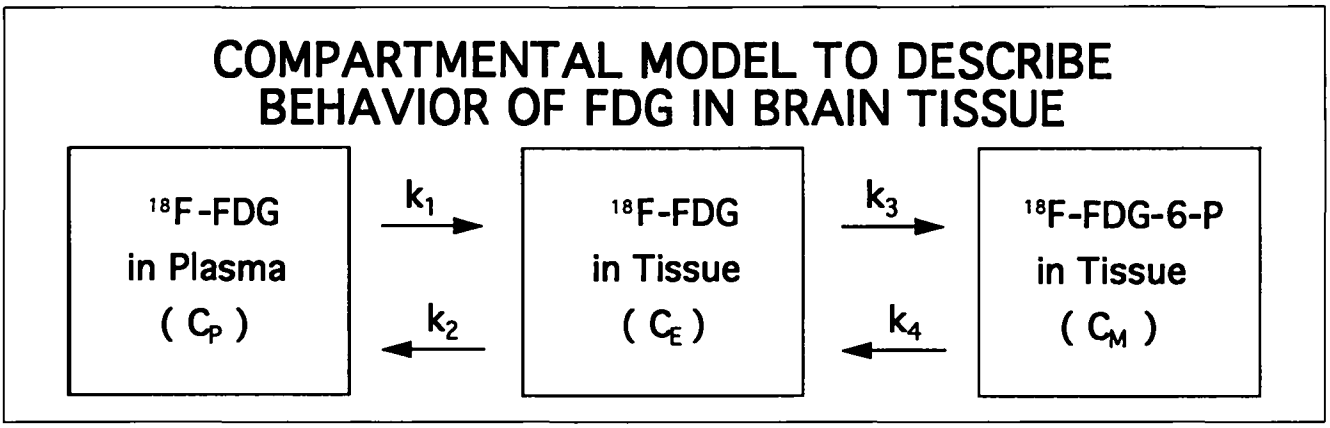

FIGURE 1. Compartmental model used to describe behavior of ^{18}F-2-fluoro-2-deoxyglucose ([^{18}F]-FDG) in brain tissue. Left compartment represents vascular space for [^{18}F]-FDG; center compartment represents tissue space for free [^{18}F]-FDG; and right compartment represents tissue space for [^{18}F]-FDG-6-phosphate. While glucose-6-P can be metabolized further, [^{18}F]-FDG-6-P can only be hydrolyzed back to free [^{18}F]-FDG. The unique rates of transfer between these compartments are represented by the constants k_1–k_4. All four rate constants are used to calculate the compartmental concentrations of $C'_E(T)$ and $C'_M(T)$ from the plasma concentration curve (C_p).

are they due to variations in methodology? The purpose of this paper was to determine the magnitude of the methodologic errors in our application of this technique.

MATERIALS AND METHODS

PET Scanner

All scans were performed using a PETT VI system (*8*). Briefly, the system uses 288 cesium flouride (CsF) detectors arranged in four rings to produce seven simultaneous tomographic slices—four straight slices and three cross slices. The system has an average intrinsic in-plane geometrical resolution of 7.1 mm full width at half maximum (FWHM) and slice thickness or axial resolution at the center of each slice of 13.9 mm FWHM. The contribution of random coincidences before correction was found to be approximately 14% of the counts in an image of a 20-cm diameter phantom containing a uniformly distributed concentration of 1 μCi/cc. An automatic method of randoms correction, based on a calculated value derived from singles count rates, was applied to all image data before analysis.

For each emission scan, a transmission scan was performed with the subject in the same position for attenuation correction using a ^{68}Ge-^{68}Ga ring source which extended beyond the field of view of the scanner.

TABLE 1
Possible Sources of Error

Variable	Error source
C_g	Accuracy and precision of plasma glucose level measurement
$C_i(T)$	Accuracy and precision of phantom sample pipetting Frequency of calibration factor calculation
C_p	Blood sampling technique Accuracy and precision of subject sample pipetting

Well Counter

Aliquots from the calibration phantom and from the subjects' plasma samples were assayed using a 90-mm diameter NaI(Tl) detector with a 25-mm diameter by 50-mm deep well connected to a single-channel pulse height analyzer. A stainless steel sleeve having a bottom and wall thickness of 0.5 mm was placed in the well to assure that all positrons annihilate prior to entering the crystal. The lower level discriminator of the pulse height analyzer was set at 355 keV with a window of 800 keV. With these settings, both singly and simultaneously detected gamma photons from positron annihilation events were recorded.

Two National Institute of Standards and Technology (NIST) traceable ^{68}Ge standards (43.12 μCi and 153.9 μCi at calibration) (Model MED3400 Gamma Reference Standards, North American Scientific, North Hollywood, CA) were used to ensure that the well counter was operating properly. Each standard was placed in the well counter and counted for one minute on each day that subject studies were performed. Pulse height analyzer settings were adjusted if the observed counts per minute for both sources were not within 5% of the expected value.

Subject Preparation

Subjects signed informed consent forms prior to participation in this study and all PET procedures were approved by the University of Chicago Hospitals' Institutional Review Board.

All subjects were instructed not to eat anything or drink beverages containing glucose or caffeine for at least four hours prior to injection so that plasma glucose levels would be relatively stable.

An individually fitted thermoplastic facemask was used to minimize subject movement and facilitate repositioning.

Each subject had an intravenous catheter placed in the proximal forearm or dorsum of the hand. The forearm and hand were then wrapped in a heating pad to increase the surface temperature of the skin to approximately 44°C. This method of arterializing venous blood has been shown to be effective and eliminates the need for arterial catheterization (*9*). The subject's arm was heated for approximately 20 min prior to injection and remained in the pad until blood sampling was completed at approximately 70 min postinjection. A second venous catheter was inserted in the opposite arm for radiopharmaceutical administration.

Immediately before each scan, subjects briefly practiced a visual monitoring task (VMT), which they would perform throughout the scanning period. The VMT consisted of the presentation of equally probable bright or dim projected white spots, occurring at random intervals of 4 to 7 sec. Subjects were instructed to press a hand-held button only in response to the dim spot. We have previously reported that this VMT produces a more controlled, stable and reproducible subject condition than that obtained when subjects were injected while awake but with their eyes covered and ears plugged (*10*).

Whenever possible, subjects were injected while in the scanner so that the arrival time of tracer in the brain could be determined.

Glucose Analysis

Glucose analysis was performed using a commercially available device which determines glucose by means of the oxygen rate method (Glucose Analyzer 2, Beckman Instruments, Inc., Brea, CA). A 10 μl sample of subject plasma was pipetted into a cup containing enzyme reagent and an electrode that responds to oxygen concentration. Within approximately 10 sec, the glucose analyzer determined the rate of oxygen consumption which is directly proportional to the concentration of glucose in the sample. The glucose concentration was then displayed in units of milligrams of glucose per 100 ml (mg/dl).

Subject glucose levels were measured at the time of injection and at 20 and 40 min after injection. The average of these three values was used for $rCMR_{glu}$ calculation.

To assess the accuracy and precision of plasma glucose level measurements, six technologists working in the PET center each performed 20 sequential determinations of a 150 mg/dl standard.

Accuracy of Pipetting

Aliquotes for counting from patient samples or the calibration phantom were prepared using a variable volume semiautomatic pipet. To assess pipetting technique, six technologists working in the PET center each performed 20 sequential pipettings of 200 μl distilled/deionized water. The weight of water delivered for each pipetting was measured using an analytic balance with a sensitivity of 0.0001 g. Each measurement was made immediately after the sample was pipetted to minimize errors due to sample evaporation.

Calibration Factor Calculations

We calculated calibration factors each day a subject study was performed using the method previously described by Phelps et al. (*9*). A 20-cm diameter phantom was filled with approximately 1 mCi of a uniformily distributed aqueous solution of ^{68}Ga (concentration approximately 0.25 μCi/ml). Prior to imaging, two 200-μl samples were removed from the phantom. Total volume of these samples was increased to 2 ml and then counted in the well counter. The phantom was then imaged. The calibration factors were obtained by dividing the decay-corrected PET scanner cps/pixel by the decay-corrected cps/ml from the sample counted in the well counter. A calibration factor was calculated for each slice. We used ANOVA of daily calibration factor calculations for a 6-mo period to determine the errors that would have resulted if new calibration factors were obtained only once a week or once a month instead of being calculated each day.

Blood Sampling Technique

To accurately define the characteristics of C_p, 1-ml blood samples were obtained at a rate of 6 to 8 per minute for the first 2 min postinjection, when C_p is changing rapidly, with additional samples obtained at 3, 4, 6, 8, 13, 18, 28, 38 and 70 min postinjection (Fig. 2). The exact time of injection (with an accuracy to the nearest whole second), sample collection and counting were recorded for each sample. The activity in each sample was then decay-corrected to the time of injection. To assess the effects of blood sampling technique, 5 subject studies were reprocessed to simulate a doubled sampling interval during the first 2 min postinjection and a missed peak (Fig. 3). The results of these reprocessed studies were compared to the original studies and a percent change was determined.

RESULTS

Our results are summarized in Table 2. The accuracy (mean/actual × 100) and coefficient of variation (standard deviation/mean × 100) for the glucose measurements were within the performance range specified for this device by the manufacturer (*11*). The accuracy and precision of our pipetting were within the recommended limits for the device being used (*12*).

DISCUSSION

We found that failing to do daily calibration factor calculations was the largest potential source of error in our study. However, it is important to recognize that this error includes the cumulative effect of pipetting accuracy, aliquot counting errors, and changes in well counter and/or scanner sensitivity. From Equation 2 we see that the 2.8% error in calibration factor calculations, that would result if new calibration factors were not obtained each day subject studies were performed, would also result in an average 2.8% error in $C_i(T)$. From Equation 3 we see that any errors in $C_i(T)$ measurement or errors due to the limits of our accuracy and

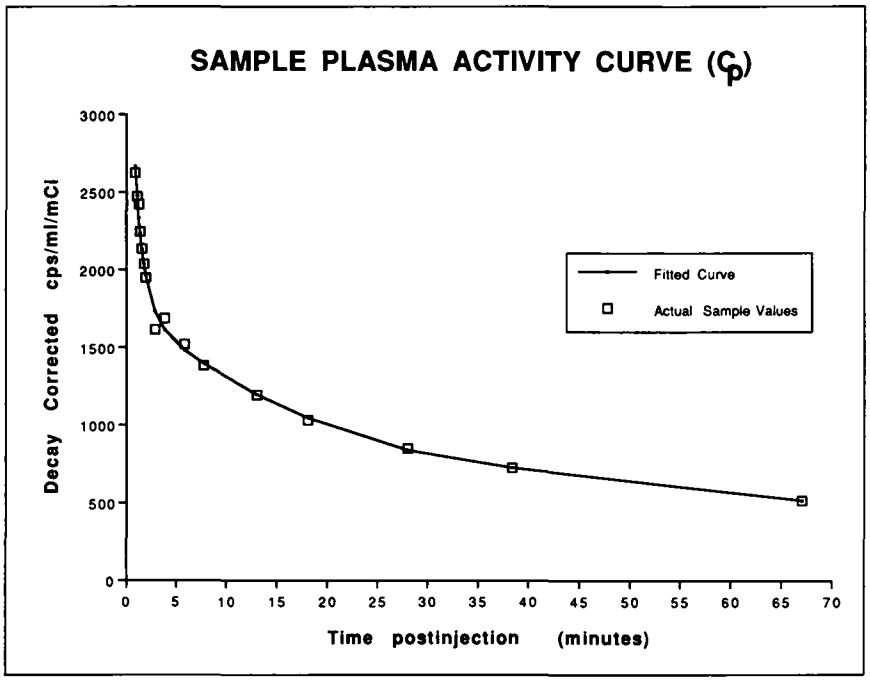

FIGURE 2. An original plasma concentration curve (C_P) fitted to a four-exponential response function. More samples are required during the first 2 min postinjection because concentrations are changing rapidly.

precision of glucose measurement will result in corresponding errors in $rCMR_{glu}$. If $C_i(T)$ or C_g are erroneously high, $rCMR_{glu}$ would be correspondingly high. Likewise, if these measurements were erroneously low, $rCMR_{glu}$ would be correspondingly low.

Even though increasing the peak count of the blood curve by 50% produces a significant change in the appearance of the blood curve, the change in $rCMR_{glu}$ was less than 1%. Similarly, doubling the sampling interval also produces a less than 1% change in $rCMR_{glu}$. This is probably because a multi-exponential equation is used to identify the line that has the best fit to the actual blood curve. The change in peak counts or a slight shift in peak time only significantly affects one exponent of this equation. This explanation is supported by Kato et al. who reported a less than 3.0% change in $rCMR_{glu}$ when the first two minutes of the blood curve were eliminated entirely (*13*). Also, since a 50% change in counts produced less than a 1.0% change in $rCMR_{glu}$, the 1.4% uncertainty in counts due to our pipetting accuracy or the 1.1% uncertainty in counts due to our pipetting precision should have an even smaller effect on $rCMR_{glu}$ calculation.

The methodological errors we have measured in this study along with errors due to subject positioning, could result in intrasubject error values on the order of 9.9% reported by

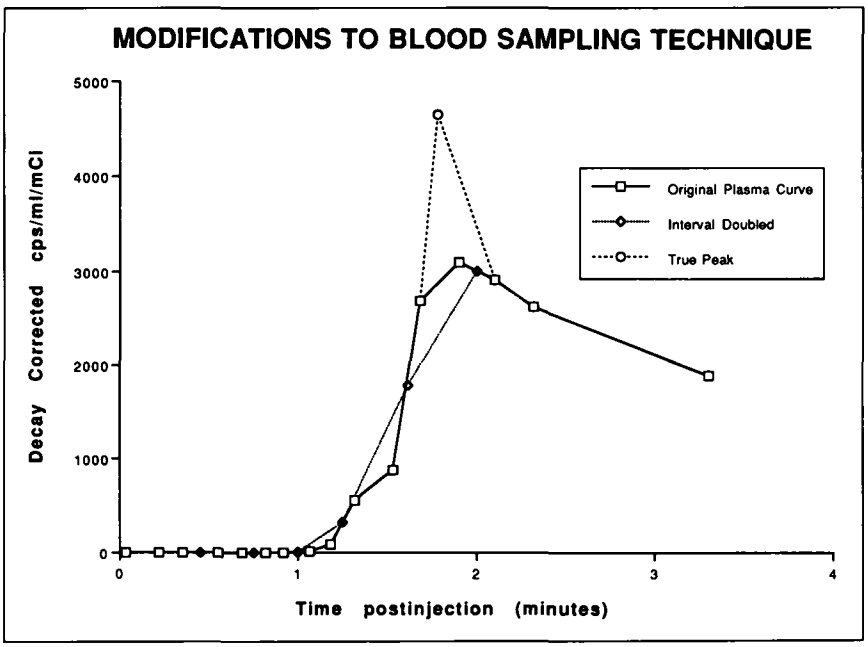

FIGURE 3. Simulated modifications to the evaluated blood sampling technique. The original curve is shown as open squares. Open diamonds show the simulated blood curve with a doubled sampling interval during the first 2 min. The average time per sample in the original study was one sample every 9 sec. In the simulated study, the interval was increased to one sample every 18 sec. Note that the result is only a slight decrease in peak counts and a slight shift to the right. The other simulated blood curve (open circles) assumes that the true peak was missed in the original curve. The simulated true peak was placed between two points of the original curve and was given a count rate 50% greater than the peak of the original curve.

TABLE 2
Methodological Error Results

Error source	Amount of error
Glucose measurement	
Average	150.5 mg/dl (Accuracy 99.7%)
Standard deviation	2.0 mg/dl (CV 1.3%)
Pipetting	
Average	197.7 μl (Accuracy 98.9%)
Standard deviation	2.8 μl (CV 1.4%)
Daily changes in calibration factors	
Coefficient of variation	2.8%
Changes in $rCMR_{glu}$ due to blood sampling technique	
Missed peak	0.7%
Doubled sampling interval	0.6%

Tyler et al. (*14*) and 7.1% reported by Camargo et al. (*15*) for repeat studies done on the same subject. A calculation of intrasubject error for the subjects in our study is not possible because each scan was performed under a different behavioral or pharmacologic condition.

CONCLUSION

The purpose of this paper was to determine the magnitude of methodological errors in our application of $rCMR_{glu}$ using PET. The largest potential source of error we found was in cross-calibration between our scanner and well counter. It is important to recognize that the stability of these cross-calibration factors will vary for each scanner and well counter combination. Other centers may encounter stability that is better or worse than what we have reported. While technologist performance of sample preparation and assaying will affect these cross-calibrations, the stability of scanner and well counter sensitivity is beyond the technologist's control. There are other aspects of scanner performance that can affect quantitative studies. These include errors in measurement of attenuation coefficients, randoms and deadtime correction, and effects of scanner spatial resolution (partial volume effect). Because these aspects of scanner performance are also beyond the control of the technologist, we did not attempt to determine their impact in this study.

It is sample preparation and assaying over which the technologist has control. As we have shown, these can introduce errors into $rCMR_{glu}$ calculation that are directly proportional to the error or variation in the process. As with the cross-calibration factors, the magnitude of these errors will be center specific. As a result, all technologists performing quantitative PET studies need to pay close attention to laboratory skills, especially proper operation and maintenance of pipettes.

In an editorial in the March 1992 issue of the *Journal of Nuclear Medicine Technology* (*16*), Drew expressed a concern regarding the adverse affects on the practice of nuclear medicine that will result if we lose our laboratory skills. The examples she gave of where these skills were required included glomerular filtration rate studies, blood volume measurements and Schilling's tests. We would add quantitative PET studies to the list of nuclear medicine procedures requiring a high degree of laboratory skill.

ACKNOWLEDGMENTS

The authors would like to thank Rita Keough for her help in editing this manuscript. This work was supported in part by the U.S. Department of Energy grant DE-FG02-86ER60438 and by the National Institute of Neurological Disorders and Stroke grant 5R01NS30400-02. This work was presented at the 39th annual meeting of the Society of Nuclear Medicine, Los Angeles, California, in June 1992.

REFERENCES

1. Engel J Jr, Henry TR, Risinger MW, et al. Presurgical evaluation for partial epilepsy: relative contributions of chronic depth-electrode recordings versus FDG-PET and scalp-sphenoidal ictal EEG. *Neurology* 1990; 40:1670–1677.
2. Jagust WJ, Friedland RP, Budinger TF. Positron emission tomography with [F-18]-fluorodeoxyglucose differentiates normal pressure hydrocephalus from Alzheimer-type dementia. *J Neurol Neurosurg Psychiatry* 1985; 48:1091–1096.
3. Martin WR, Stoessl AJ, Adam MJ, et al. Positron emission tomography in Parkinson's disease: glucose and DOPA metabolism. *Adv Neurol* 1987; 45:95–98.
4. Hutchins GD, Holden JE, Koeppe RA, et al. Alternative approach to single-scan estimation of cerebral glucose metabolic rate using glucose analogs, with particular application to ischemia. *J Cereb Blood Flow Metab* 1984;4:35–40.
5. Sokoloff L, Reivich M, Kennedy C, et al. The [C14] deoxyglucose method for the measurement of local cerebral glucose utilization: theory, procedure, and normal values in the conscious and anesthetized albino rat. *J Neurochem* 1977;28:897–916.
6. Berman M. Kinetic models for absorbed dose calculations. *MIRD Pamphlet Number 12*. New York, NY: Society of Nuclear Medicine; 1977.
7. Huang SC, Phelps ME, Hoffman EJ, et al. Noninvasive determination of local cerebral metabolic rate of glucose in man. *Am J Physiol* 1980;238: E69–E82.
8. Ter-Pogossian MM, Ficke DE, Hood JT Sr, et al. PETT VI: a positron emission tomograph using cesium fluoride scintillation detectors. *J Comput Assist Tomogr* 1982;6:125–133.
9. Phelps ME, Huang SC, Hoffman EJ, et al. Tomographic measurement of local cerebral glucose metabolic rate in humans with [F18]2-fluoro-2-deoxy-D-glucose: validation of method. *Ann Neurol* 1979;6:371–388.
10. Cooper MD, Metz JT, Kalbhen C, et al. Metabolic characterization of brain states: opposing effects of partial sensory limitation on left and right brain responses [Abstract]. *J Nucl Med* 1989;30:899.
11. Brown D. *Beckman glucose analyzer 2 operating manual*. Brea, CA: Beckman Instruments, Inc.; 1983.
12. Nickoloff EL and Thorell JI. A hospital program for radioimmunoassay quality control. In: Rhodes BA, ed. *Quality control in nuclear medicine*. St. Louis, MO: C. V. Mosby; 1977:397–408.
13. Kato A, Menon D, Diksic M, et al. Influence of the input function on the calculation of the local cerebral metabolic rate for glucose in the deoxyglucose method. *J Cereb Blood Flow Metab* 1984;4:41–46.
14. Tyler JL, Strother SC, Zatorre RJ, et al. Stability of regional cerebral glucose metabolism in the normal brain measured by positron emission tomography. *J Nucl Med* 1988;29:631–642.
15. Camargo EE, Szabo Z, Links JM, et al. The influence of biological and technical factors on the variability of global and regional brain metabolism of 2-[F-18]fluoro-2-deoxy-D-glucose. *J Cereb Blood Flow Metab* 1992;12: 281–290.
16. Drew HH. In my opinion [Editorial]. *J Nucl Med Technol* 1992;20:1.